Photonic network laser

Heeso Noh,[1,*] Jin-Kyu Yang,[1] Seng Fatt Liew,[1] Michael J. Rooks,[1] Glenn S. Solomon,[2] and Hui Cao[1,3]

[1]*Department of Applied Physics, Yale University, New Haven, Connecticut 06511, USA*

[2]*Joint Quantum Institute, National Institute of Standards and Technology and University of Maryland, Gaithersburg, Maryland 20899, USA*

[3]*Department of Physics, Yale University, New Haven, Connecticut 06511, USA*

**Corresponding author: heeso.noh@yale.edu*

Received April 19, 2011; revised August 16, 2011; accepted August 17, 2011; posted August 17, 2011 (Doc. ID 146187); published September 8, 2011

We demonstrated lasing in two-dimensional trivalent network structures with short-range order. Despite the lack of translational and rotational symmetries, such structures possess a large isotropic photonic bandgap. Different from those of a photonic crystal, the band-edge modes are spatially localized and have high quality factor. © 2011 Optical Society of America

OCIS codes: 250.5960, 230.5298.

As an optical analog to the amorphous solid, a photonic amorphous structure (PAS) has no translational or rotational symmetry but short-range order on the length scale of the optical wavelength. There are two types of topology: (i) an aggregate of dielectric spheres/cylinders and (ii) a continuous network of dielectric material. Previous studies demonstrate that a photonic bandgap (PBG) can be formed in (i) via coupling of Mie resonances of individual scatterers [1–6]. Recently, two-dimensional (2D) and three-dimensional (3D) realizations of (ii) have been shown to possess even larger PBGs [7–9]. For example, a photonic amorphous diamond structure formed by a 3D network of silicon has an 18% PBG [8,9]. Since the PAS is isotropic, the PBG is identical in all directions. The photonic band-edge (BE) modes can be strongly localized without intentionally introducing any defect in a PAS [6,7,9]. It is dramatically different from a periodic structure where the PBG is anisotropic and the BE modes are spatially extended.

Most studies on amorphous network structures have focused on passive systems that have no gain or nonlinearity. Little is known of the active structures. In this Letter, we introduce optical gain to the 2D amorphous network structures and demonstrate lasing with optical pumping. The lasing modes are the BE modes that are strongly confined and have high quality (Q) factor.

To generate a 2D trivalent network structure (each junction having three bonds), we first created a jammed packing of polydisperse cylinders in a computer simulation [10]. The center positions of the cylinders are marked by black solid circles in Fig. 1(a). Then we performed a Delaunay tessellation that provides triangular partitioning (blue thin lines) [7]. Associated with each triangle is a centroidal point. We connected the centroids of neighboring triangles with line segments. The resulting structure is a trivalent network shown by the red thick lines. The spatial Fourier spectra of the structure [inset of Fig. 1(b)] exhibits a circular ring pattern, indicating that the structure is isotropic and there exits a dominant spatial frequency that corresponds to the radius of the ring. We also calculated the 2D spatial correlation function $C(\Delta r)$, which is plotted in Fig. 1(b). The characteristic length scale of the structure a is obtained from the first peak of the correlation function. The rapid decay of the amplitude of $C(\Delta r)$ with Δr reveals the structural correlation is short ranged.

As to be detailed later, we fabricated 2D trivalent network structures in a GaAs membrane that was 190 nm thick and free standing in air. To obtain the effective index of refraction n_e of the GaAs segments for the 2D simulation, we computed the fundamental PBG in a triangle lattice of air holes in a free-standing GaAs membrane (using the plane wave expansion method), then adjusted n_e of an approximate 2D structure to get a similar PBG. The value of n_e depends on the filling fraction of air in the GaAs membrane f, which is chosen to be 0.53 to have the maximal PBG. The 2D network structure was assigned the same $f = 0.53$ and $n_e = 2.68$. We calculated the 2D density of optical states (DOS) using the order N method in a finite-difference time-domain (FDTD) simulation [11]. The boundary condition is periodic, and the supercell contains 2048 vertices. Only TE modes are considered, as the lasing modes in the GaAs membrane are TE polarized due to stronger amplification by quantum dots (QDs). Figure 1(c) displays a significant depletion of the DOS in the 2D trivalent network. For comparison, we calculated the DOS for an amorphous array of monodisperse air cylinders in GaAs. This structure was derived from the jammed packing of polydisperse cylinders (from which the network structure was created) by reducing the radii of all cylinders to a constant value. The air filling fraction f is identical to that in the network structure. As is seen in Fig. 1(c), the DOS has only a shallow dip in the amorphous array of air cylinders. Hence, the PBG effect is greatly enhanced in the trivalent network structure. This is attributed to the uniform topology of each junction.

Next we calculated the quality factor ($Q \equiv \omega\tau$, ω is the frequency, τ is the lifetime) of the resonant modes in the 2D structure with the finite-element method (using the commercial software COMSOL). The network has 2048 vertices and an open boundary. As shown in Fig. 1(d), there are no guided modes with TE polarization in the frequency range $a/\lambda = 0.32$ and 0.38, as a result of the complete PBG for TE guided modes. The highest-Q modes are located at the BEs. They are tightly confined within the structure, as seen in Figs. 1(e) and 1(f). The spatial localization of BE modes reduces light leakage

 © 2011 Optical Society of America

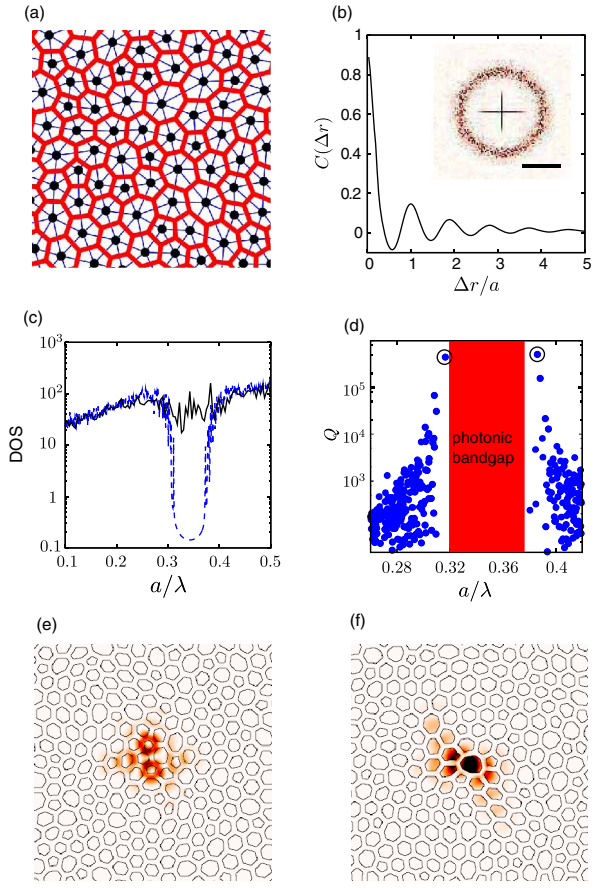

Fig. 1. (Color online) (a) Black solid circles are the center positions of polydisperse cylinders produced by jammed packing in a computer simulation. The blue thin lines represent the Delaunay tessellation that leads to the formation of a trivalent network structure shown by the red thick lines. (b) Spatial Fourier spectra (inset) and spatial correlation function $C(\Delta r)$ (main panel) of the trivalent network structure (scale bar: $2\pi/a$). (c) Calculated density of optical states for a trivalent network structure (blue dashed curve) and an amorphous array of air cylinders (black solid curve) with the same air filling fraction $f = 0.53$ and dielectric refractive index $n_e = 2.68$. (c) Calculated Q factor of the resonant modes in the trivalent network structure as a function of the normalized frequency a/λ. (e) and (f) are calculated intensity distributions of two modes [circled in (d)] at the low and high frequency sides of the bandgap.

through the boundary of the structure, resulting in a high Q factor. This is distinct from the periodic structure whose BE modes are extended. Figures 1(e) and 1(f) also reveal that the intensity of the BE mode at the low/high frequency side of the PBG is mostly concentrated in the dielectric/air. Thus it can be labeled the dielectric/air BE mode.

The computer-generated patterns of the 2D trivalent network were transferred to a GaAs membrane containing InAs QDs. Figure 2(a) is a top-view scanning electron microscope (SEM) image of one pattern with $a = 315\,\text{nm}$. The lateral dimension of each pattern is $9.7\,\mu\text{m} \times 9.7\,\mu\text{m}$. A series of patterns with different a were fabricated. The lasing experimental setup is the same as that in [10]. Briefly, a mode-locked Ti:sapphire laser (pulse width ~200 fs, center wavelength ~790 nm, pulse repetition rate ~76 MHz) is used to excite the InAs QDs.

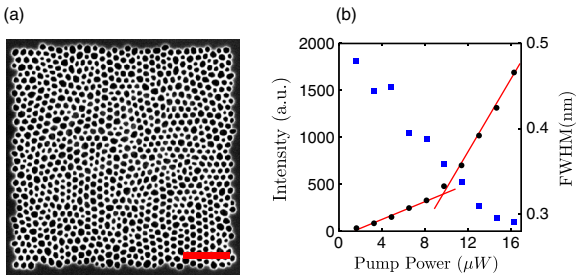

Fig. 2. (Color online) (a) Plane-view SEM image of the fabricated trivalent network structure in a GaAs membrane with $a = 315\,\text{nm}$. The scale bar is $2\,\mu\text{m}$. (b) Measured intensity (black circles) and spectral width (blue squares) of one emission peak at $\lambda = 1000\,\text{nm}$ as a function of the incident pump power P.

The pump spot is about $3\,\mu\text{m}$ in diameter. The emission is collected from the top by an objective lens for spatial imaging and spectral analysis.

We realized lasing in a network structure of $a = 315\,\text{nm}$ with optical excitation of InAs QDs. The emission spectrum consisted of a few narrow peaks on top of a broad background [top curve in Fig. 3(a)]. The background originated from the broadband amplified spontaneous emission, while the narrow peaks corresponded to the resonant modes. Figure 2(b) plots the intensity of one emission peak at wavelength $\lambda = 1000\,\text{nm}$ versus the incident pump power P. It displayed a threshold behavior. When P exceeded $9.8\,\mu\text{W}$, the emission intensity increased much more rapidly with P. The FWHM of the peak also decreased dramatically with increasing P and reached the value of 0.28 nm at $P = 16\,\mu\text{W}$. Such behaviors indicate the onset of lasing action. The optical image of the lasing mode, shown in Fig. 4(a), reveals that the mode was located in the interior of the pattern. Its lateral size was approximately $2.4\,\mu\text{m}$, significantly smaller than the pattern size ($9.7\,\mu\text{m}$). With a further increase of pump power, we observed lasing in multiple modes.

We repeated the lasing experiment on different network configurations with the same a. They were generated from different jammed packings of polydisperse cylinders. Their spatial Fourier spectra and spatial correlation functions were nearly identical, indicating that these configurations are statistically equivalent. Lasing was realized in these patterns within the same spectral range, although the frequencies of individual lasing modes varied from pattern to pattern [Fig. 3(a)].

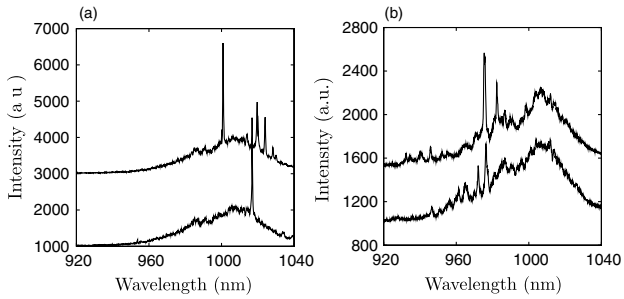

Fig. 3. Measured emission spectra for the trivalent network structures of (a) $a = 315\,\text{nm}$ and (b) 275 nm. The two spectra in each panel are taken from different configurations. With decreasing a, the lasing modes blueshift.

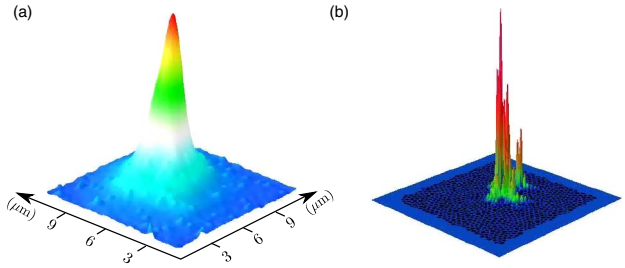

Fig. 4. (Color online) (a) Optical image of the lasing mode in Fig. 2(b). (b) Spatial intensity distribution of the dielectric BE mode calculated in a 3D FDTD simulation of the real structure.

We performed 3D FDTD simulation of the real structures that were extracted from the digitized SEM images. The results illustrated that the lasing modes were located near the dielectric BE of the PBG. The air BE was located at much shorter wavelength $\lambda \simeq 720\,\mathrm{nm}$. The air BE modes could not lase as they were beyond the gain spectrum of the InAs QDs. Although they can be tuned into the gain spectrum by increasing a, the dielectric BE modes are preferred for lasing as they are concentrated in the GaAs and experience more gain from the InAs QDs. We calculated a dielectric BE mode in the 3D FDTD simulation. As shown in Fig. 4(b), the mode was spatially localized and had a size similar to the measured one in Fig. 4(a). However, the fine features, e.g., closely spaced intensity maxima, were smeared out in the optical image due to a finite resolution of our imaging system. The Q factor of this mode was about 6000, which was limited by the out-of-plane leakage of light.

Finally we probed lasing in trivalent network structures of different a. Figure 3(b) displays the emission spectra taken from two configurations of $a = 275\,\mathrm{nm}$. Lasing peaks shift to shorter wavelength. This move is consistent with the blueshift of the dielectric BE as a decreases. However, the 3D FDTD calculation predicted that the dielectric BE would shift to $\lambda \sim 900\,\mathrm{nm}$, but the lasing peaks were seen around 975 nm. Although the dielectric BE modes at 900 nm had higher Q, they were far from the peak of gain spectrum and experienced much lower gain than the modes at 975 nm. Thus, the latter had a lower lasing threshold and dominated the lasing spectra.

In conclusion, we fabricated 2D trivalent network structures with short-range order in a free-standing GaAs membrane. Despite the lack of long-range order, such structures displayed wide isotropic photonic bandgaps. We realized lasing in the dielectric BE modes with optical pumping. The BE modes were spatially localized, different from the extended BE modes in photonic crystals. The lasing frequencies depended not only on the structural correlation length, but also on the spectral position of optical gain. By varying the characteristic length scale of the network structure, we could tune the lasing frequency within the gain spectrum of QDs. Since it has only short-range order, the PAS may be fabricated by self-assembly, which is much easier than the standard nanofabrication of the photonic crystal laser, especially in 3D.

We thank Professor Corey S. O'Hern and Carl Schreck for useful discussion and computer generation of jammed packings of polydisperse cylinders. This work is funded by National Science Foundation (NSF) Grants DMR-0808937 and PHY-0957680. J.-K. Yang acknowledges the support of the Korea Science and Engineering Foundation (KOSEF) through the Grant for the Photonics Integration Technology Research Center (R11-2003-022) at the Optics and Photonics Elite Research Academy.

References

1. C. Jin, X. Meng, B. Cheng, Z. Li, and D. Zhang, Phys. Rev. B **63**, 195107 (2001).
2. J. Ballato, J. Dimaio, A. James, and E. Gulliver, Appl. Phys. Lett. **75**, 1497 (1999).
3. C. Rockstuhl, U. Peschel, and F. Lederer, Opt. Lett. **31**, 1741 (2006).
4. Y. Wang and S. Jian, Phys. Lett. A **352**, 550 (2006).
5. C. Rockstuhl and F. Lederer, Phys. Rev. B **79**, 132202 (2009).
6. M. Rechtsman, A. Szameit, F. Dreisow, M. Heinrich, R. Keil, S. Nolte, and M. Segev, Phys. Rev. Lett. **106**, 193904 (2011).
7. M. Florescu, S. Torquato, and P. J. Steinhardt, Proc. Natl. Acad. Sci. USA **106**, 20658 (2009).
8. K. Edagawa, S. Kanoko, and M. Notomi, Phys. Rev. Lett. **100**, 013901 (2008).
9. S. Imagawa, K. Edagawa, K. Morita, T. Niino, Y. Kagawa, and M. Notomi, Phys. Rev. B **82**, 115116 (2010).
10. J.-K. Yang, C. Schreck, H. Noh, S.-F. Liew, M. I. Guy, C. S. O'Hern, and H. Cao, Phys. Rev. A **82**, 053838 (2010).
11. C. T. Chan, Q. L. Yu, and K. M. Ho, Phys. Rev. B **51**, 16635 (1995).